World Conference on Timber Engineering Oslo 2023

# DESIGNING AND TESTING OF A WOOD-ONLY TIMBER FRAME CONNECTION INSPIRED BY THE GROWTH FORMATION OF TREES' STEM-BRANCH JUNCTION

**Firas Hawasly[1], Naoyuki Matsumoto[2], Mikio Koshihara[3], and Koji Adachi[4]**

**ABSTRACT:** This paper presents the design approach and testing of a new column-beam connection utilising wood as the sole structural material for application in multi-storey timber frames. This connection was inspired by the all-wood natural formation of trees' stem branch junction model. The growth model features were explored and approached in a simplified application of glued-laminated column-beam members joined through a conical mortise-tenon interface with bent laminated veneer plies flowing seamlessly across the connection. The tested connection was compared to steel-added conventional joint systems resulting in a comparable bending performance with desirable ductile behaviour and presenting the inclusion of seamless bent timber members as a possible reinforcement against bending for timber connections.

**KEYWORDS:** Bio-inspired, Tree growth, Seamless fibres flow, Bentwood reinforcement

## 1 INTRODUCTION

The current application of steel and concrete in rigid frame structures is an appealing canvas for architectural applications, providing flexibility, uniformity, and safety; it is an evolved form of the long and rich history of timber framing, overcoming the span limitations and the inherent material combustibility.

The reappreciated potentiality of wood as a construction material following the shortages of iron through the world wars, combined with the awareness of the environmental impact of the construction field, facilitated an expedited shift in timber engineering research [1, 2] to maximise the utilisation of timber products in structural applications. However, and to a certain extent, it was applied by simply substituting the less sustainably sourced and widely utilised concrete and steel members with timber, using the same structural vocabulary, theory, and detailing, and expecting structural behaviour similar to that of the designed and manufactured materials.

In contrast, trees grow wood through 'Morphogenesis' [3], a form generation, adaptive growth process where the material properties are manipulated whilst waste and energy are optimised to ensure maximum functionality and efficiency and create a fully localised functional and structural system. Nevertheless, the adaptive growth processes of a tree, being complicated and ingenious natural systems (e.g., deviation of grain patterns, shedding of branches, encasing of knots), are, however, considered defects when the wood is used as a structural material. The techniques used in modern timber engineering depend on segregating these tree-specific, homogeneous structural tissues. Contrary to the early building traditions, wood was fitted to the desired location based on its form in the tree and guaranteed structural performance, e.g., shipbuilding.

The limitations imposed by the structural capabilities of the segregated, reused, linear, natural material and the limitation in the sourcing processes introduced a myriad of engineered timber products with enhanced structural properties; and have constantly been challenged by the feasibility of achieving an efficient joining system. As a result, a broad spectrum of innovative connections for timber was developed utilising processes and materials foreign to the organic wood. They fulfilled the sought structural requirements while gradually shifting the naturally grown material into a normalised product to suit our growing understanding of timber structures away from the systems and analytical tools initially developed for the designed concrete and steel materials.

While sharing a similar morphology to a timber frame connection, the trees' stem-branch junctions are inherently moment resistant; these cantilevered protrusions resist moments generated at their junctions by self-weight and wind loads [4]. This growth formation is nature's manifestation of wood as a constructional material, an intricately generated form that contributes to the tailored structural behaviour in resisting bending, shear, and fatigue induced by static and dynamic loads. Hence, investigating and mimicking its distinct and specific growth processes is sought to introduce a further befitting constructional language of timber at frame connections.

[1] Firas Hawasly, Institute of Wood Technology, Akita Prefectural University, hawasly_firas@iwt.akita-pu.ac.jp
[2] Naoyuki Matsumoto, Department of Architecture and Building Science, Graduate School of Engineering, Tohoku University, nmatsu@rcl.archi.tohoku.ac.jp
[3] Mikio Koshihara, Institute of Industrial Science, The University of Tokyo, kos@iis.u-tokyo.ac.jp
[4] Koji Adachi, Institute of Wood Technology, Akita Prefectural University, kadachi@iwt.akita-pu.ac.jp


https://doi.org/10.52202/069179-0186

In this paper, biomimetic investigations of load paths and fibre assemblies of stem-branch junctions in trees inspired an approach towards a wood-only utilisation of a structural entity capable of transferring bending loads safely within a timber frame joint.

## 2 GROWTH FORMATIONS AT TREE BRANCH JUNCTIONS

The secondary growth of trees occurs at the vascular cambium, a thin, active layer of cells that forms a continuous sheath beneath the plant's surface. It increases the thickness of the plant seasonally in concentric layers by division outwards and inwards, creating phloem and xylem tissues, respectively. Xylem tissues, which make the whole woody material from longitudinal tube-like fibrous cells, are responsible for the tree's stability and the transfer of sap in one direction between the roots and leaves; given the energy and waste optimisation, there is no functional requirement, nor structural, for the fibres to flow from the branch up the stem or to other branches.
A single growth layer in a branch can be modelled as a unidirectional, fibrous, double-bent surface; hence, the growth model of a tree is interpreted as a stack of concentric, fibrous, unidirectional, double-bent surfaces. (Figure 1-1). Geometrically, the interface between the surfaces of the stem and the branch is conical and, depending on the branch's growth vigour, is partially or fully encased within the flow of the stem's fibres [5].
At the ridge point, the branch's fibres exhibit a sharp turn with small radii whilst maintaining their conductive functionality and gradually easing towards the junction's lower section in alignment with the stem. Similarly, the upper stem's fibres flow around the branch collar and exhibit similar radii above the branch ridge. Trees utilise the unidirectional flow of the branching fibres to create tissues with interlocking geometric assemblies at the top portion of the branch's collar to prevent failure and damage. These tissues are stiffer and mechanically superior to normal wood, albeit with constricted conductive functionality as a "structural trade-off" to support this critical location.[5, 6]. Furthermore, the naturally optimised form of the stem combined with the residual tensile stresses of its natural growth (preloading) significantly improve the tree's strength [7] and, consequently, the transfer of loads across the junction. [8]
In this paper, the explored growth model features of a branch junction are:

- the uninterrupted, seamless flow of fibres across the junction,
- the complicated compressed fibre formations within the conical interface of the junction, and
- the variable mechanical properties of localised wood cell types across the junction.

### 2.1 Hypothetical growth model

As the flow of forces in biological materials is governed by the direction of the fibres [9], trees transfer gravity and wind loads along the fibres from the leaves to the roots; additionally, the tree acquires an adequate resistance of uplift loads through the geometric fibres' assembly across the junction.
However, the frame structural connections demand substantial horizontal resistance. Hence, a hypothetical growth model was developed, assuming trees were designed to resist uplift and gravity loads equally by alternating the fibres' flow direction every other growing season, resulting in an equal cross-sectional area of the stem below and above the branching point. (Figure 1-2) (Contrary to Leonardo da Vinci's rule stating that the sum of the cross-sectional area of fibres above the branching point is equal to that below it)However, although this loading pattern contradicts the wood's natural growth and function, it is expected to provide the sought performance in resisting loads in both directions.

### 2.2 Simplification process

The current limitations in wood sourcing and machining technologies hinder the ability to produce a double-bent unidirectional surface similar to the interpreted model of a growth layer from wooden veneer material, especially with the localisation of different cell types (reaction, opposite and normal wood). Therefore, to utilise simple

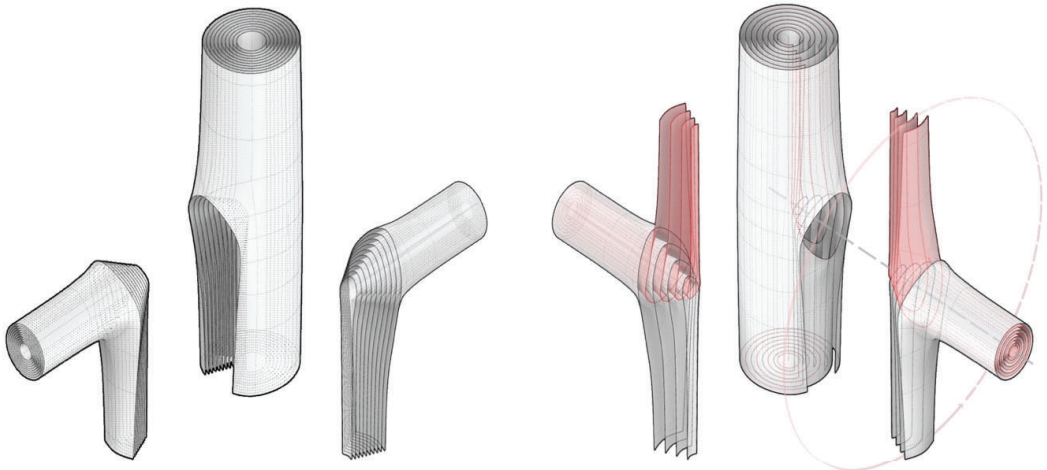

***Figure 1:*** *Interpreted and hypothetical growth models of Stem-branch junction; (left) a detached branch showing the conical interface of the successive growth layers; (right) a detached view of the hypothesized branch through flipping every other growth*

https://doi.org/10.52202/069179-0186

techniques and available wood products, the proposed approach oversimplified the hypothetical growth model into two applicable connection patterns:
- Bent fibre continuity as a stack of one-way bent veneers in a T-formation, where the fibres are seamlessly flowing from the stem to one half of the branch (Figure 1-2), and
- Concentric fibre connectivity as a stack of concentric tubular veneers, where the fibres of corresponding tubes are butt-jointed, resulting in a stepped conical mortise-tenon integration (Figure 1-3).

## 3 MATERIALS AND METHODS

The approached connection combines both simplified interpretations of the hypothetical model, utilising the conical interface of a glued, stepped mortise-tenon beam integration within the column (Figure 1-6), with a set of symmetrical bent plies flowing seamlessly from the beam across the interface and into both directions of the column (Figure 1-5).
For this application, the dimensions were based on a selected prototype of a generic medium-sized office building with a simple and flexible structural system developed by 'KI' "www.ki-ki.info" (a Japanese timber structural study group and database) to promote and provide technical information for one-way timber frame structures using standardised glued-laminated timber sections for columns and beams at 600x210mm E65-F225 JAS (Japanese Agricultural Standards) in Japanese Cedar (*Cryptomeria japonica)*. In addition, two steel-added

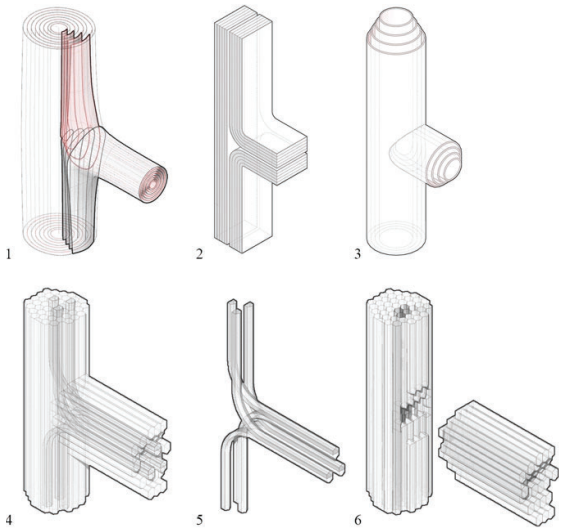


***Figure 2:*** *Simplification and proposed connection typology; 1. hypothetical branch model; 2. bent fibre continuity; 3. concentric fibre connectivity; 4. connection morphology; 5. seamless bent plies; and 6. conical interface*

conventional joint systems were experimentally and numerically tested for this prototype in Japanese Cedar at half width (600x105mm), namely the glued-in rod (GIR) [10] and the lag-screw bolts (LSB) [11].

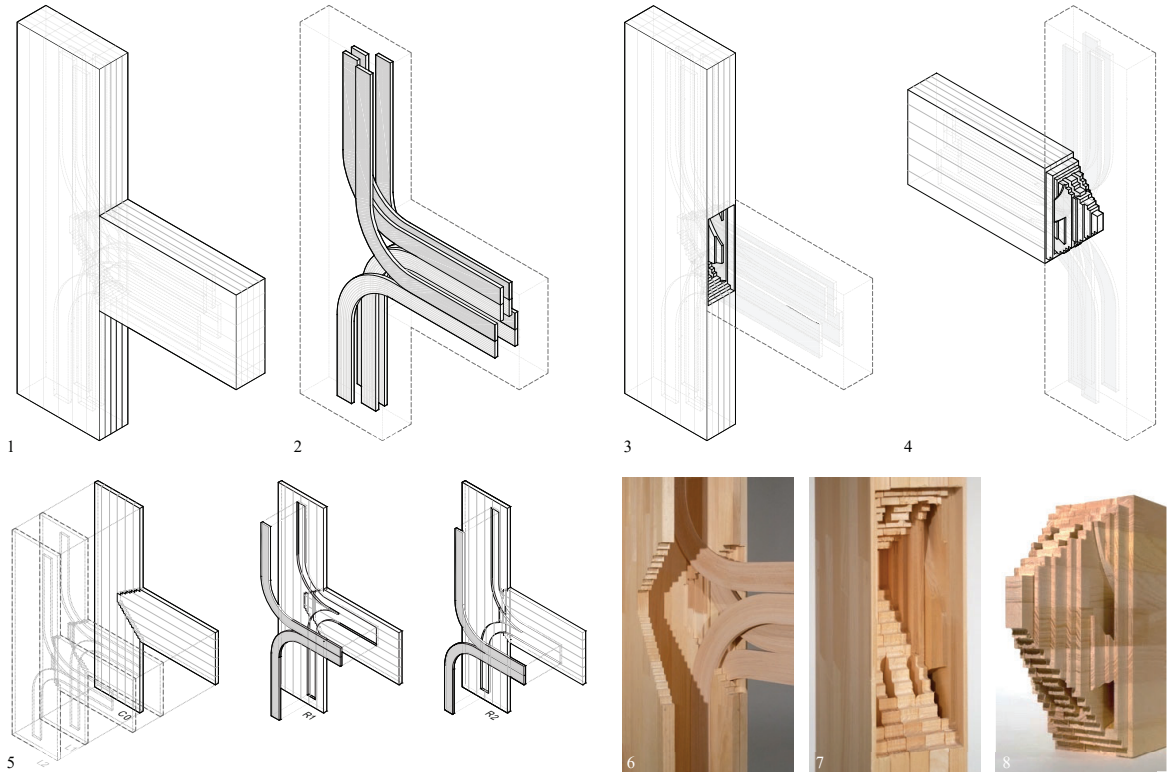


***Figure 3:*** *The proposed connection (1); exploded isometric view of the constituting elements: bent plies (2), column (3), and beam(4); placement of the bent plies within the carved channels in the glue-laminated column-beam lamellae (5), a dry fit of the Pine column with the bent plies in their corresponding channels (6); and the conical interface in the column (7) and the beam (8)*


https://doi.org/10.52202/069179-0186

### 3.1 DESIGN DEVELOPMENT

Given the symmetrical and volumetric features of the multi-member integration, the size of the tested connection was opted to maintain the original proportions at half scale (300x105mm). Through the lamination process of the five laminated column-beam pairs, eight bent plies were fitted within corresponding channels placed symmetrically along the horizontal and vertical axes of the pair C0 (which contains no channels), flowing seamlessly from the beam and into both directions of the column. (Figure 3). The column-beam members were manufactured in Japanese Cedar (*Cryptomeria japonica)* and Merkusii Pine (*Pinus merkusii*), whereas the included seamless plies were manufactured from bent-laminated veneers in Beech (*Fagus crenata*).

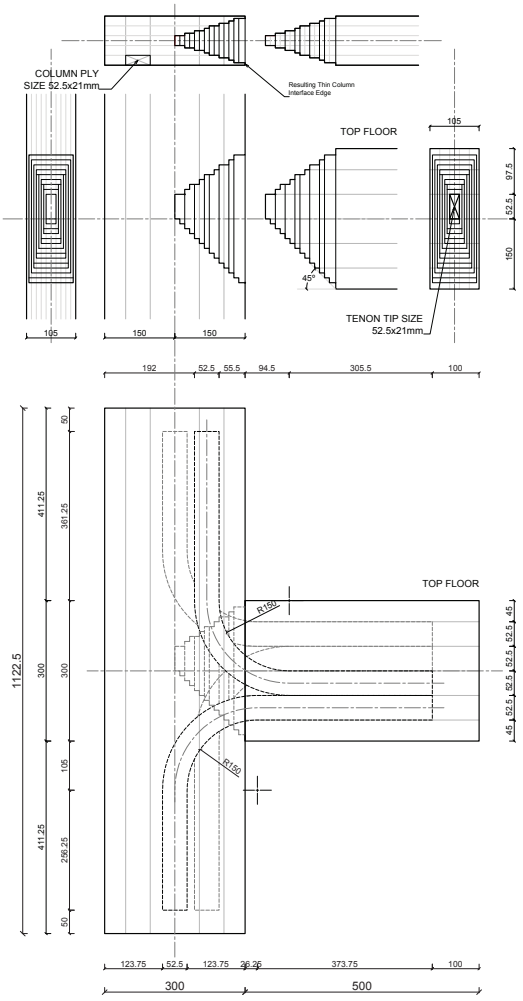


***Figure 4:*** *Sizing of the conical interface without channels (above) and the column-beam assembly with the placement of the included bent plies (bottom) (units in mm)*

The detailed sizing of the connection was based on a 10.5mm module per half the thickness of a single laminated column-beam pair at 300x21mm; the boards were made from edge-glueing six 52.5x21mm plies and were cut to a finished length of 1122.5mm and 650mm, for the column and beam, respectively.

The conical interface initiated above the column-beam axes' intersection with a single ply (at 52.5x21mm) and stepped towards the entire cross-section of the beam on a 10.5mm cubic grid. (Figure 4 - the asymmetrical interface mimics the shifted axis of the branch integration, a geometric growth feature of the flow of fibres)

Both sides of the column-beam members were processed with a CNC machine to shape the conical interface and carve the 52.5x10.5mm channels for the bent plies. The 90º fit at the edges of the conical interface and channels were processed with relief cuts at the inner corners using a Ø6mm bit. (Refer to Figure 9-left)

The bent plies were made from 90x1x1200mm Beech veneers, and they were bent-laminated with an inner radius of 150mm to a 54mm nominal thickness with aqueous polymer isocyanate adhesive (Koyo-Bond KR-134 at 150gm-2 spread) in block forms and cured under a press at 0.65MPa for 4 hours. Next, eight plies were rip-cut on a bandsaw at 10.5mm width and re-fitted to the desired channel (due to glue-bending spring-back) with ±1.5mm tolerance on a CN machine to a final section of 52.5x10.5mm; and a 3mm radius fillet was added to the edges facing the channels for glue distribution. Finally, the assembly of the connection members in Cedar and Pine was performed using resorcinol formaldehyde resin (Dianol 33N at 150gm-2 spread) and cured under a press at 1.0MPa for 6 hours. Moreover, a column-beam assembly without the channels for the included Beech plies was manufactured in Cedar and Pine to isolate the reinforcement effect of including the bent plies on the bending performance.

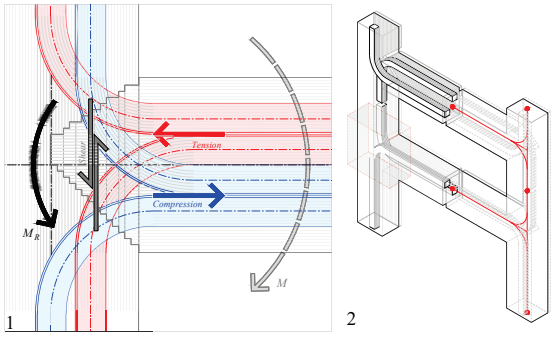


***Figure 5:*** *The schematic structural dynamics of the proposed connection in response to an applied bending moment (1) in the proposed pinned portal frame system typology (2)*

### 3.2 PROPOSED STRUCTURAL DYNAMICS

The modern applications of timber frame joints utilise adding foreign elements (to wood) at joint locations to provide the required resistance against specific loads. (primarily steel, e.g., plates and pins for shear, bolts and tie-rods for tension, and lags and threaded rods for bending) In contrast, the developed system approaches the features of the all-wood natural formation at branch locations through the above-mentioned simplified models in response to the hypothesised loading conditions.

Like the conical branch integration within the stem, the column-beam conical interface distributes shear loads evenly across its faces and reduces concentrated embedment damages. At the same time, the axial transfer

https://doi.org/10.52202/069179-0186

of compressive and tensile loads through the seamless bent plies reinforces the bending and shear performances due to their integration within the conical interface. as illustrated in (Figure 5-1).
Furthermore, the members are manufactured from species with different initial properties that, combined with the resulting multi-directional fibre assemblies, contribute to the approached distribution of mechanical properties; however, unlike trees, it is non-homogenous.
The proposed typology of the structural system utilises a one-way pinned-portal frame, similar to the monopodial nature of trees. [4, 12] (Figure 5-2)

## 4 TEST SETUPS AND RESULTS

The tests in this study focused on the static bending performance of the used materials and components.

### 4.1 THREE-POINT BENDING TEST

The bending performance of the Cedar, Pine, and laminated Beech plies was evaluated with a three-point bending test spanning 350mm. Table 1 lists the averaged dimensions, moduli of elasticity and rupture, with the initial stiffness derived from the tests and the initial modulus of elasticity acquired through a stress wave velocity measurement (utilising a *Fakopp* microsecond timer).

### 4.2 BENDING TEST OF BENT PLIES

The bending performance of six bent-ply specimens was tested in the setup displayed in Figure 6. The plies were laid horizontally and through-pinned on equal distances from the arched portion to the test base at one end and to an actuator at the other; given their slender sections, Teflon sheets separated the plies from the sandwiching steel plates with rollers to suppress the out-of-plane deformations.
Four specimens were loaded cyclically in the push (close) and the pull (open) directions, and two were loaded monotonously in either direction. The setup mimics the loading condition of the plies within the column-beam members in push (close) and pull (open) strokes. The cyclic deformation values were 1, 2, 3.5, 5, 7.5, 10, 15, and 20mm with 5mm increments till failure at a rate of 1mm per minute, corresponding to 750, 375, 200, 150, 100, 75, and 50 rad$^{-1}$ of deformation angle as derived by equation (1):

$$\Theta = 2\,tan^{-1}\left[d \,/\, 2a\sqrt{2} - d\right] \qquad (1)$$

Where $\Theta$ is the deformation angle, $d$ *is* the linear displacement between pins, and $a$ is the 45° projection of the distance between the pins (refer to Figure 6).
Table 2 lists the averaged initial stiffness $K_0$, the maximum load $P_{max}$ in the push (close) and the pull (open) directions, and the resulting bending moment mid-span of the arched section [$M_{max}=P_{max}\,(H + h/2)$], with the corresponding linear displacement $d_{max}$ and the deformation angle $\Theta_{max}$.
As illustrated in the load-displacement curves of four samples loaded till failure in the push (close) and pull (open) cycles (Figure 7), the bent plies exhibited higher ductility in the cyclic push direction and failed with

***Table 1:*** *Three-point bending test results (values in paratheses are the standard deviation)*

| Material | n | *b* mm | *h* mm | *l* mm | $E_{Fakopp}$ kN/mm$^2$ | *MoE* kN/mm$^2$ | *MoR* N/mm$^2$ | $K_0$ N/mm |
|---|---|---|---|---|---|---|---|---|
| Cedar Single Ply | 6 | 28.0 | 29.0 | 640.8 | 7.2 (1.4) | 8.2 (1.1) | 58.3 (6.9) | 158.3 (23.6) |
| Pine Single ply | 3 | 27.0 | 30.0 | 832.5 | 11.9 (1.9) | 12.0 (2.8) | 58.1 (14.2) | 218.4 (62.8) |
| Beech Laminated Ply | 6 | 24.5 | 10.5 | 445.5 | 10.7 (0.7) | 10.2 (0.4) | 83.5 (3.3) | 140.9 (6.6) |

*where* *b and h are the section dimensions; l, the length of the specimen; $E_{Fakopp}$, Initial modulus of elasticity; MoE, modulus of elasticity in; MoR, modulus of rupture; $K_0$ initial stiffness*

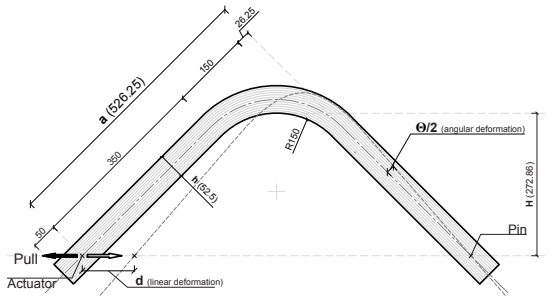


***Figure 6:*** *Bending test setup for Beech bent plies (units in mm)*

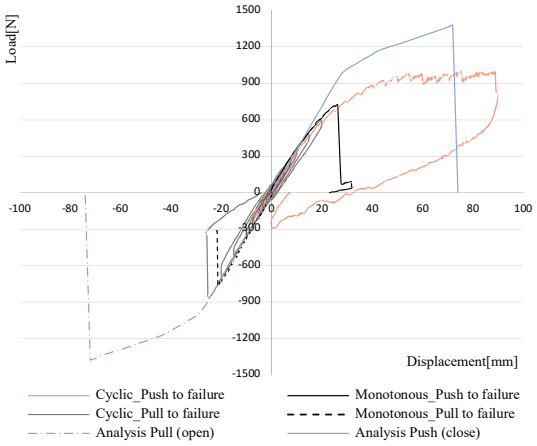


***Figure 7:*** *Load-displacement curves in four tested bent plies in the push (close) and pull (open) directions and the analysed approximation*

***Table 2****: Bent plies bending test results*

| Stroke | n | $K_0$ N/mm | $P_{max}$ N | $d_{max}$ mm | $\Theta_{max}$ $10^{-3}$ rad | $M_{max}$ kN.m |
|---|---|---|---|---|---|---|
| Push close | 5 | 33.7 (1.0) | 770.5 (210.0) | 40.6 (27.4) | 56.8 (39.5) | 0.23 0.063 |
| Pull pull | 5 | 35.6 (0.9) | 584.4 (208.3) | 16.2 (6.1) | 21.5 (8.0) | 0.17 0.062 |

*where* *$K_0$, initial stiffness; $P_{max}$ maximum load and its corresponding $d_{max}$ linear displacement, $\Theta_{max}$ angular deformation, and $M_{max}$ bending moment at the middle of the arched portion*


https://doi.org/10.52202/069179-0186

gradual crack development, while they failed in brittle behaviour when loaded in the pull direction.
The concentrated axial forces in the pull (open) cycles initiated failures near the centroidal axis with fibrous fracture patterns; these cracks gradually grew through the glue lines towards the pins, whereas the concentrated compressive forces excreted by the push (close) cycles were translated to fibre kinks on the concave side and tensile fracture on the concave side with out-of-plane deformations (twisting). However, the bent plies included in the full joint assembly will be glued within carved channels, effectively acting as a clamping feature and minimising the lateral deformation while maximising the tensile and shear strengths of the laminated material.

### 4.3 BENDING TEST OF THE COLUMN-BEAM ASSEMBLIES

The bending performance of the column-beam members with the included bent plies and without the channels for the bent plies (only the conical interface) was evaluated under a cyclic displacement-based loading protocol with values derived from the total frame drift. Table 3 lists the variations of the ten tested connections regarding the column-face support, the inclusion of bent plies, and material, in addition to an assembly in Cedar with a modified conical interface as a characteristic value. [CBRc with rigid column-face support had the central pair C0 of the column-beam lamella flipped, providing a larger glueing surface area and an extended tenon - Figure 9]
The loading was applied once per cycle till failure through an actuator pinned to a steel plate fixed at the upper side (top floor) of the vertical beam; the column face was laid on the test base with rigid or pin supports at its face and rigid supports at the ends, as shown in Figure 8. The different face support conditions were tested to investigate the performance of the second half of the column, given the placement of the bent plies along its centroidal axis.
Additionally, two horizontal supports with spherical rollers were added near the centre of the beam's surface to suppress out-of-plane deformations.
The cyclic angular deformation values in the push and pull directions were 300, 200, 150, 75, 50, 30, and 20 rad$^{-1}$ at a rate of 1mm per minute. The loading was maintained until the load was reduced to 70% of the maximum load or till failure. The moment-rotation angle envelopes of the cyclic hysteresis loops in the push (compression) and pull (tension) directions for the Pine and Cedar variations are illustrated in Figure 10 and Figure 11, respectively. The data and derived evaluation items from the performed tests are listed in Table 3.

### 4.4 SIMPLIFIED ANALYTICAL MODEL

The comprising members of the connection, i.e., the eight bent plies and the five pairs of column-beam lamellae, were approximated analytically as a combination of individual models of beam-elements (Figure 13), simulating the support and loading conditions of the rigidly supported connection assemblies of PBR and CBR using Midas-iGen. (a general-purpose structural analysis and optimal design system)

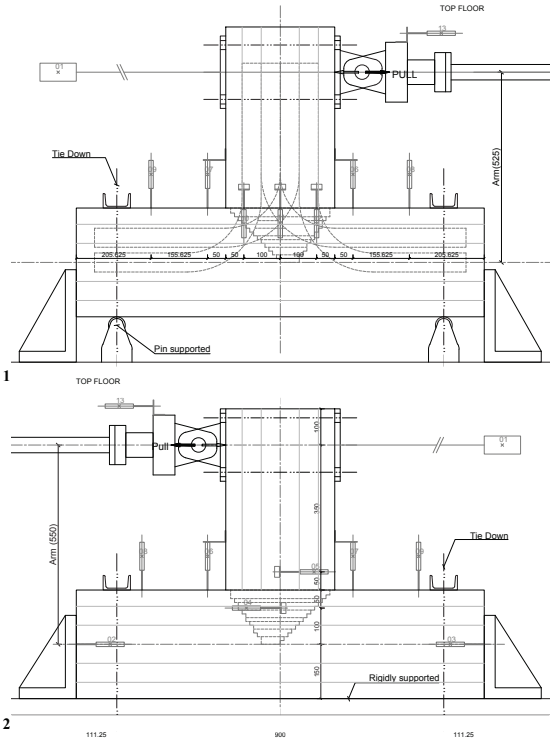


***Figure 8:*** *Column-beam assemblies test setups. 1. Front side of the pin-supported full connection, and 2. Back sided of the rigidly supported column-beam assembly. Both setups share the same placement of transducers (1~13) (units in mm)*

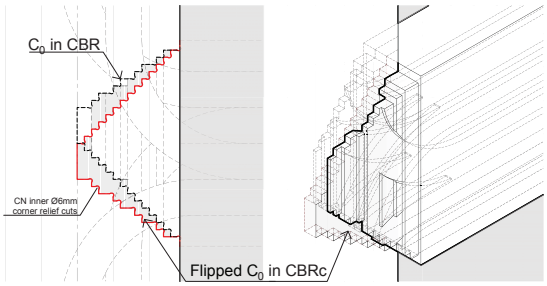


***Figure 9*** *Details of the flipped C0 in the conical interface of CBRc; hatched areas represent the added gluing surface of the extended tenon (left: illustrates the CN Ø6mm relief cuts)*

The arched portion of the bent ply was modelled in five rigidly connected linear beam-elements (Figure 12-1) with isotropic material properties derived from the three-point bending tests. Each segment had an elastic performance with a plastic hinge (equal to the material's yield strength $P_y$) near its rigid connections. The simulation followed the bent plies bending tests in support and loading conditions (results are illustrated in Figure 7, noting that the included bent plies were loaded within the plastic region in the column-beam assemblies)
Similarly, the centre-lines of the column-beam members were modelled as two linear beam-elements joined with a rotational spring (Figure 12-2). The spring properties were derived from the sole performance of the conical interface in the column-beam assembly without the bent plies PWR and CWR.

https://doi.org/10.52202/069179-0186

***Table 3:*** *Results of bending tests of column-beam and full connection assemblies*

| Material | Name | Bent Plies | Column-face | Number | | $M_{max}$ kNm | $M_y$ kNm | $M_u$ kNm | $M_{1/150rad.}$ kNm | $\delta_{max}$ $10^{-3}$rad | $\delta_y$ $10^{-3}$rad | $\delta_v$ $10^{-3}$rad | $K_0$ kNm/rad | $K_s$ kNm/rad | $\mu$ - | $D_s$ - |
|---|---|---|---|---|---|---|---|---|---|---|---|---|---|---|---|---|
| Merkusii Pine | PWR | Without | Rigid | 1 | Push | 16.5 | 8.6 | 14.8 | 16.1 | 7.0 | 4.33 | 4.04 | 4146.6 | 3675.6 | 3.12 | 0.44 |
| | | | | | Pull | 14.4 | 10.1 | 13.5 | 13.6 | 9.0 | 4.07 | 3.57 | 4118.4 | 3786.9 | 2.85 | 0.46 |
| | | | | | Ave. | 15.5 | 9.4 | 14.2 | 14.9 | 8.2 | 4.20 | 3.80 | 4132.5 | 3731.2 | 2.98 | 0.45 |
| | PBR | With | Rigid | 1 | Push | 35.1 | 18.0 | 29.0 | 21.8 | 12.0 | 2.34 | 8.33 | 3699.9 | 3475.0 | 1.42 | 0.74 |
| | | | | | Pull | 31.2 | 19.3 | 31.7 | 22.2 | 14.0 | 2.68 | 8.62 | 3381.9 | 3671.3 | 1.96 | 0.59 |
| | | | | | Ave. | 33.2 | 18.6 | 30.3 | 22.0 | 13.1 | 2.51 | 8.48 | 3540.9 | 3573.1 | 1.69 | 0.66 |
| | PBP | With | Primed | 2 | Push | 25.9 | 15.6 | 22.7 | 15.59 | 16.19 | 6.61 | 9.67 | 2494.1 | 2349.4 | 2.77 | 0.47 |
| | | | | | Pull | 26.0 | 16.6 | 24.0 | 15.33 | 16.21 | 7.58 | 10.90 | 2329.4 | 2210.0 | 2.01 | 0.58 |
| | | | | | Ave. | 26.0 | 16.1 | 23.4 | 15.46 | 16.20 | 7.10 | 10.28 | 2411.7 | 2279.7 | 2.37 | 0.53 |
| Japanese Cedar | CWR | Without | Rigid | 1 | Push | 10.3 | 6.2 | 9.6 | 9.8 | 11.0 | 3.03 | 4.68 | 2361.7 | 2047.8 | 2.82 | 0.46 |
| | | | | | Pull | 9.2 | 5.8 | 8.1 | 8.5 | 8.0 | 2.26 | 3.18 | 2574.2 | 2550.1 | 4.26 | 0.36 |
| | | | | | Ave. | 9.7 | 6.0 | 8.8 | 9.1 | 9.8 | 2.60 | 3.93 | 2467.9 | 2299.0 | 3.54 | 0.41 |
| | CBR | With | Rigid | 2 | Push | 16.0 | 10.0 | 14.2 | 11.3 | 11.7 | 5.12 | 7.32 | 2079.2 | 1944.2 | 4.11 | 0.37 |
| | | | | | Pull | 14.3 | 11.5 | 13.2 | 10.9 | 10.5 | 7.24 | 8.35 | 1663.1 | 1582.8 | 2.44 | 0.52 |
| | | | | | Ave. | 15.1 | 10.7 | 13.7 | 11.1 | 11.1 | 6.18 | 7.84 | 1871.2 | 1763.5 | 3.22 | 0.45 |
| | CBRc* | With | Rigid | 1 | Push | 19 .5 | 10.5 | 18.2 | 15.0 | 14.0 | 5.17 | 7.49 | 2607.9 | 2430.1 | 2.34 | 0.52 |
| | | | | | Pull | 19.7 | 10.2 | 17.9 | 14.7 | 13.9 | 5.26 | 7.15 | 2549.9 | 2505.6 | 2.25 | 0.54 |
| | | | | | Ave. | 19.6 | 10.4 | 18.1 | 14.9 | 13.9 | 5.22 | 7.32 | 2578.9 | 2467.9 | 2.29 | 0.53 |
| | CBP | With | Primed | 2 | Push | 15.6 | 10.5 | 15.3 | 11.3 | 13.9 | 5.58 | 8.14 | 1860.1 | 1888.8 | 3.21 | 0.43 |
| | | | | | Pull | 16.4 | 9.6 | 14.8 | 10.9 | 15.7 | 5.62 | 8.71 | 1694.8 | 1700.5 | 3.14 | 0.47 |
| | | | | | Ave. | 16.0 | 10.1 | 15.1 | 11.1 | 14.8 | 5.60 | 8.42 | 1777.5 | 1794.6 | 3.17 | 0.45 |

* CBRc with a modified conical interface (refer to Figure 9)

*where* *M, moment; δ, angular deformation; K, stiffness; μ, Ductility factor; Ds, structural characteristic factor; subscripts; max, Maximum; y, Yield; u, Ultimate; v, yield point; 0, Initial; s, Secant; 1/150, Load corresponding to the angular deformation angle of 1/150 radian.*

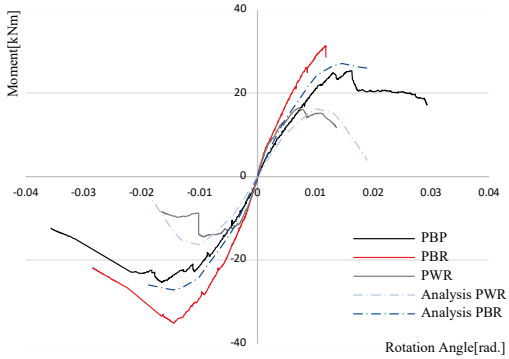


***Figure 10:*** *Moment-rotation angle envelope curves in tested and analysed Pine variations*

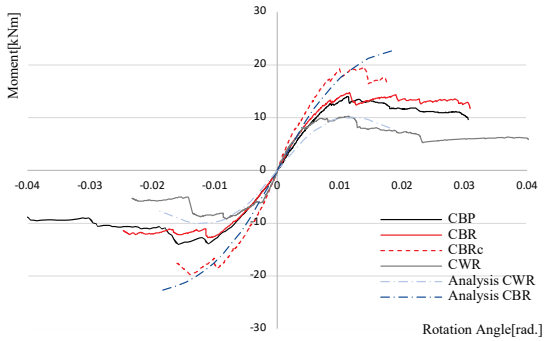


***Figure 11:*** *Moment-rotation angle envelopes curves in tested and analysed Cedar variations*

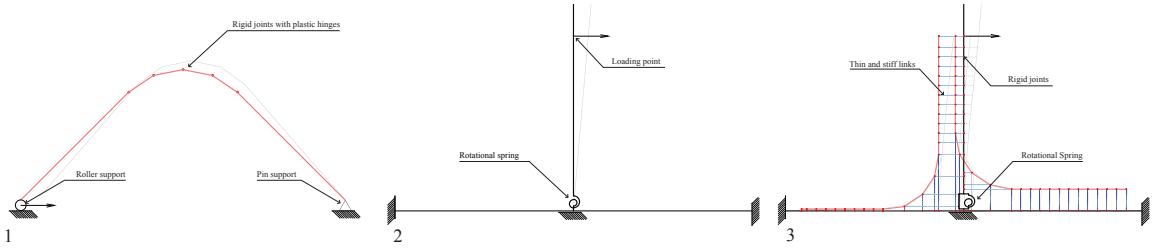


***Figure 12:*** *Analytical beam models of the connection members, 1. bent ply model (in push/close), 2. C0 with a rotational spring (in push), 3. R1\|L1(in push) and R2\|L2 (in pull) combining both models with stiff and thin links accounting for the captive channels*


https://doi.org/10.52202/069179-0186

The conical integration of the beam within the column changes in size across its section, where the central lamina (C0) has the maximum integration. Ideally, the rotational spring should be weighted according to its integration when included in the model of each lamina; however, for simplification, the spring capacity was divided equally across the five laminae, given that the whole connection's analytical result is the sum of its members.

On the other hand, the linear segments of the bent plies were rigidly connected to the nearest column-beam element with thin and stiff links at 30mm intervals, whereas the segmented arched portion was connected to the column and beam elements. (Figure 12-3)

Accordingly, and given the connection's symmetry (where L1|R1 and L2|R2 are mirrored copies), the simplified analytical model of the connection in the push direction is the sum of $[C0_{push}+2L1_{push}+2L1_{pull}]$

The analytical models' performance of the column-beam assembly (without the channels for the bent plies) and the whole connection are illustrated in Pine and Cedar in Figure 10 and Figure 11, respectively.

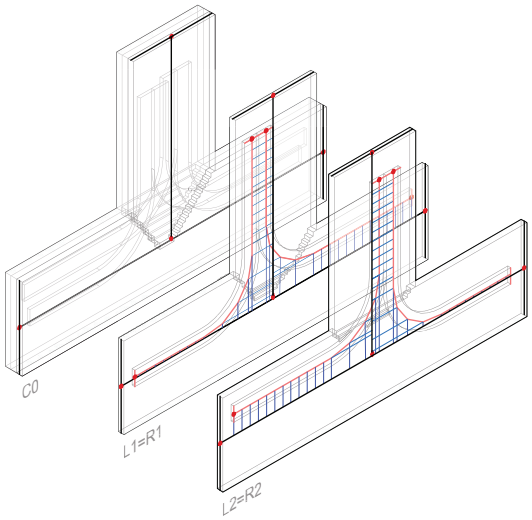


***Figure 13:*** *Beam element models of the whole connection as the sum of the performance of the individual laminae models* $[C0_{push}+ 2L1_{push} + 2L1_{pull}]$

## 5 DISCUSSION

In all tested variations, early cracks were observed at the finger-joined plies of the glue-laminated boards at the thin edge of the column interface. Additionally, dissecting the connection's conical interface showed that the butt-jointed glue faces perpendicular to the loading plane were weakened by the CN machining corner relief cuts (Figure 14); moreover, the failure of the included bent plies was limited to splitting failure at the centroidal axis.

In the column-beam assemblies (without the bent plies, CWR and PWR), the distributed shear loads across the faces of the conical interface reduced the embedment of the tenon; however, the separation at the relief cuts and the conical geometrical slope caused the beam to pull out due to the cyclic loading, at which the connection was secured by the shear performance of the glue in the stepped surfaces parallel to the loading plane. (Figure 14)

Compared to the sole performance of the conical interface in PWR, including the bent plies in the Pine variations, PBR and PBP achieved a 114% and 68% increase in the maximum moment and a 14% and 42% decrease in the initial stiffness, respectively.

Similarly, the Cedar variations CBR and CBP achieved a 56% and 65% increase in the maximum moment and a 24% and 28% decrease in the initial stiffness compared to CWR, respectively.

However, CBRc with the modified conical interface exhibited the best performance, increasing the maximum moment by 102%, 23%, and 18% and the initial stiffness by 4%, 27%, and 31% compared to CWR, CBR, and CBP, respectively. Since the middle lamella of the conical interface (C0) does not contain any channels and is immediately glued to neighbouring bent plies, flipping its direction in BRc created an extended tenon. It increased the total glueing surface area by 20%, reinforcing the initial stiffness and moment capacity of the whole assembly while reducing the ductility factor; nonetheless, it failed in a similar pattern.

Furthermore, the bent plies acted as shear keys due to their integration within the asymmetrical conical interface, reduced the initial stiffness, prevented the beam from pulling out, and concentrated splintering and interlaminar failures along the vicinity of the conical interface and transverse tensile failure at the central region of the column along their linear axes (Figure 15).

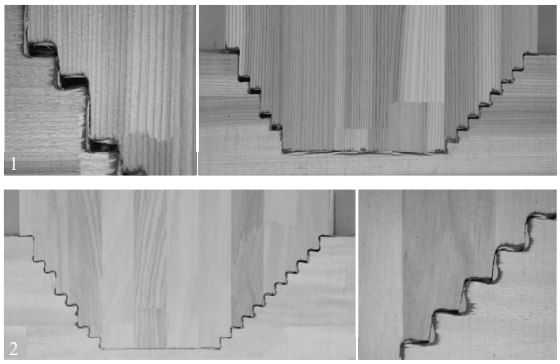


***Figure 14:*** *Pull-out and relief cut separation in a dissected conical-interface in Cedar (1) and Pine (2)*

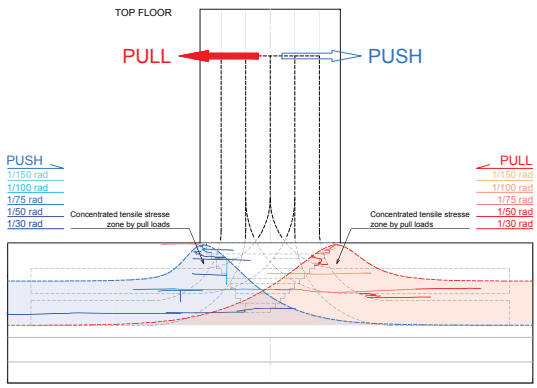


***Figure 15:*** *Zone of the concentrated tensile stresses due to the included bent plies (cracks shown are from a CBR variation)*

https://doi.org/10.52202/069179-0186

However, due to the termination of the beam and bent plies integrations at the column's axis, the lower half was not fully incorporated in resisting the increased tensile stresses of the combined performance of the included bent plies and their captive channels. As a result, the performance of the pinned and rigidly supported connections was comparable in the Cedar variations; however, it was pronounced in the Pine variations (due to its higher MoE); additionally, vertical cracks in the PBP's beam were observed.

## 5.1 COMPARISON WITH STEEL-ADDED CONNECTIONS

Based on the calculation methods provided for the glued-in rod (GIR) [10, 13] and the lag-screw bolt (LSB) [11] at 105x600mm, the initial stiffness and ultimate loads were derived for a 105x300mm GLT section. Table 4 lists the ultimate moment and the initial stiffness of the compared connections. Figure 16 illustrates the equivalent energy elastic-plastic (EEEP) bilinear models averaged in the push and pull directions, the moment-rotation angle envelopes of tested variations, and the projected performance of GIR and LSB.

Accordingly, CBRc achieved a similar moment capacity to GIR with a reduced initial stiffness and an increased ductility (given the brittle failure pattern of GIR); on the other hand, it exceeded LSB's initial stiffness with a reduced moment capacity. Additionally, it has a joint efficiency of 30%, a practical value for a moment resisting joints in timber structures [14], calculated by Equation(2):

$$\alpha = M_{max}/F_b \times Z \quad (\times 100\%) \qquad (2)$$

Where α, joint efficiency; Mmax, maximum moment; Fb, bending strength of the glue-laminated member (= 27.5 N.mm$^{-2}$ based on the "Japanese Agricultural Standard for Glued laminated timber 2007"); and Z, section modulus of the glulam member at 105x300mm.

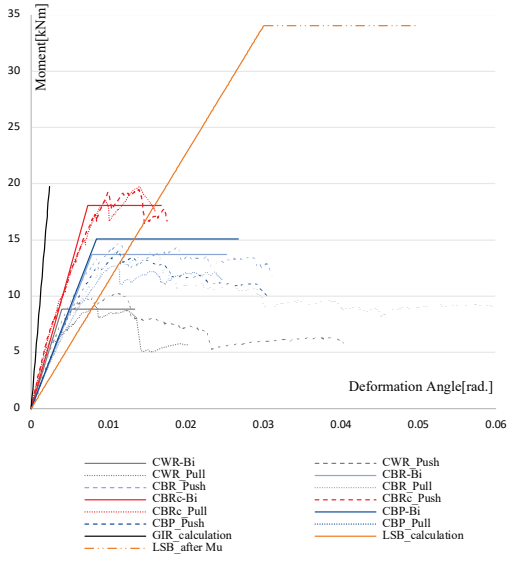


***Figure 16*** *Moment-Rotation envelopes and the averaged bilinear models of all tested variations in comparison to the calculations of LSB & GIR in Cedar (at 105x300mm)*

***Table 4*** *Comparison with GIR and LSB [values in brackets are relative to CBRc]*

| Theme | Name | $K_0$ Initial Stiffness kNm.rad$^{-1}$ | - | $M_u$ Ultimate Moment kNm | - |
|---|---|---|---|---|---|
| Wood-only Bio-inspired | CWR | 2467.9 | [96%] | 8.8 | [49%] |
| | $CBR_{ave}$ | 1871.1 | [73%] | 13.7 | [76%] |
| | CBRc | 2578.9 | [100%] | 18.1 | [100%] |
| | $CBP_{ave}$ | 1777.5 | [69%] | 15.1 | [83%] |
| Steel-added Conventional | GIR | 8325.6 | **[323%]** | 19.8 | [109%] |
| | LSB | 1134.4 | [44%] | 34.0 | **[188%]** |

## 5.2 PARAMETRIC INVESTIGATION

Further investigation in the material combinations was analysed in Cedar in CWR and CBR variations with enhanced material properties as parameters, as follows:

- Column-beam materials: modulus of elasticity *MoE.*
- Conical interface: rotational spring capacity in stiffness *K*, maximum load $P_{max}$, and yielding load $P_y$.
- Bent plies: modulus of elasticity *MoE* and yielding load $P_y$ at the hinges.

Table 5 lists the analysed parametric variations, and Table 6 lists the correlations of the maximum moment and stiffness in the parametric and tested variations.

The enhanced material and rotational spring in the column-beam assembly without the bent plies in C2B0R achieved a similar maximum moment and a 57% increase in stiffness in CBRc, whereas C2B1R doubled the initial stiffness and maximum moment in CBR. On the other hand, the enhanced bent plies in C1B2R approached the effect of the elongated conical interface in CBRc, which complies with the tested impact of the bent plies on the shear performance of the conical interface.

***Table 5:*** *Analysed parametric variations*

| | | Beech (Bent Plies) | | |
|---|---|---|---|---|
| | | B0 | B1 *1 x MoE, Py* | B2 *2 x MoE, Py* |
| Cedar (Column-Beam) | C1 *1xMoE, Pmax, Py, K* | C1B0R *(=CWR)* | C1B1R *(=CBR)* | C**B2**R |
| | C2 *2xMoE, Pmax, Py, K* | C2B0R | **C2**B1R | **C2B2**R |

***Table 6:*** *Correlations of the maximum moment [above the diagonal] and stiffness [below the diagonal] in the analysed parametric variations*

| | | | $M_{max}$ [kNm] | | | Moment at 0.015 rad[kNm] | | | |
|---|---|---|---|---|---|---|---|---|---|
| | | | CWR | CBR | CBRc | **C2**B0R | C1**B2**R | **C2**B1R | **C2B2**R |
| | | | 9.7 | 15.1 | 19.6 | 20.19 | 22.61 | 34.39 | 41.95 |
| Stiffness [kNm.rad$^{-1}$] | CWR | 2299 | 1 | 1.56 | 2.02 | 2.08 | 2.33 | 3.55 | 4.32 |
| | CBR | 1763.5 | 0.77 | 1 | 1.30 | 1.34 | 1.50 | 2.28 | 2.78 |
| | CBRc | 2467.9 | 1.07 | 1.00 | 1 | 1.03 | 1.15 | 1.75 | 2.14 |
| | **C2**B0R | 2769.3 | 1.20 | 1.57 | 1.12 | 1 | 1.12 | 1.70 | 2.08 |
| | C1**B2**R | 2693.2 | 1.17 | 1.53 | 1.09 | 0.97 | 1 | 1.52 | 1.86 |
| | **C2**B1R | 3681.2 | 1.60 | 2.09 | 1.49 | 1.33 | 1.37 | 1 | 1.22 |
| | **C2B2**R | 4144.4 | 1.80 | 2.35 | 1.68 | 1.50 | 1.54 | 1.13 | 1 |


https://doi.org/10.52202/069179-0186

## 6 CONCLUSION

Given that the proposed structural system was based on and limited by the dimensions of the case study and the currently available simple manufacturing technologies, the performance achieved by the bio-inspired, only-wood connection competed with the conventional steel-added joints and presented the utilisation of bent timber members within the frame joints as a possible application for reinforcement against bending moments, inviting further explorations and inspirations from tree structures. The parametric analysis (approximated from the material perspective) provided insights into the different material effects; however, further investigations into the adhesive properties and the geometric design in terms of configuration, size and dimensions are equally important. Furthermore, the proposed system had a long and complicated manufacturing process in controlled factory conditions compared to the simple in-situ application of the steel-added joint systems. Hence, further developments and simplifications for integrating and manufacturing these approaches are required, especially considering the design and assembly of multi-directional seamless members within two-way frame systems.

Although this research presented a valid proposal for the application of wood connections in timber frames in light of its performance in static bending and judging by the failure patterns, it can be argued whether the only-wood applications are supposed to seek a rigid performance comparable or similar to the steel-added ones. Regarding the projected shortcomings and limitations of the wood material in the current structural and constructional applications compared to its superiority and suitability in its natural formation, addressing the concept of damping in timber frames instead of rigidity is expected to provide further insights into timber structures towards a befitting constructional language in structural applications.


## ACKNOWLEDGEMENT

- This work was partially supported by 'The Ministry of Education, Culture, Sports, Science and Technology (MEXT) Scholarship' and the 'Japan Society for the Promotion of Science - JSPS KAKENHI Grant number: JP22K20463'.
- Part of this work was submitted to the 'AIJ Journal of Technology and Design (Architectural Institute of Japan)" and was presented at the '73rd Annual Meeting of the 'Japan Wood Research Society (JWRS)'.


## REFERENCES


[1] Bell P. W. R.: Wooden Structures by G. G. Karlsen and the Derevyagin beam. In: *History of Construction Cultures*, London, 734–740, 2021

[2] Arlet J. L.: Innovative Carpentry and Hybrid Joints in Contemporary Wooden Architecture. Arts, 10(3):64, 2021

[3] Thompson D. W.: On growth and form. Cambridge University Press, 2014

[4] Grigorian M.: Biomimicry and theory of structures-design methodology transfer from trees to moment frames. Journal of Bionic Engineering, 11(4):638-648, 2014

[5] Slater D.: An argument against the axiom of uniform stress being applicable to trees. Arboricultural Journal, 38(3):143-164, 2016

[6] Hu M., Olsson A., Hall S., and Seifert T.: Fibre directions at a branch-stem junction in Norway spruce: a microscale investigation using X-ray computed tomography. Wood Science and Technology, 56(1):147–169, 2022

[7] Pasini D. and Burgess S. C.: Optimal structural features in trees and their application in engineering. In C.A. Brebbia and L.J. Sucharov, editors, *Design and Nature*, pages 3–15. WIT Press, United Kingdom 2002

[8] Burns L. A.: Bio-Inspired Design of Aerospace Composite Joints. RMIT University, 2012

[9] Mattheck C.: Design in Nature. Springer Berlin Heidelberg, Germany, 1998

[10] K. Tanaka et al.: Study on Strength Mechanism of Joint System Using Metal Connector and Adhesive in Timber Structures Part.23 Consideration of Calculating Method for Bending Performance of Beam-Column Joint Using GIR Joint. (in Japanese), In *Summaries of the 2021 AIJ Annual Convention,* 421–422, 2021

[11] K. Tsuboi et al.: Basic Study on Lag-screw-bolt Connection Performance for Mid-rise Timber Construction. (in Japanese), In *Summaries of the 2021 AIJ Annual Convention*, 413–414, 2021

[12] Hawasly F., Matsumoto N., and Koshihara M.: Bio-Inspired Wood-Only Timber Frame Joint Typologies Based on the Seamless Fiber Continuities of a Tree's Stem-Branch Junction. In *Summaries of the 2021 AIJ Annual Convention*, 873–876, 2021

[13] Sato K. et al.: Study on Strength Mechanism of Joint System: Using Metal Connector and Adhesive in Timber Structures Part.21 Horizontal Loading Test for Moment Resisting Performance of Beam-Column Joint with Shear Key Considering Ease of Construction. (in Japanese) In *Summaries of the 2021 AIJ Annual Convention*, 417-418, 2021

[14] Nakata K. and Komatsu K.: Development of Timber Portal Frames Composed of Compressed LVL Plates and Pins II. Strength properties of compressed LVL joints as moment resisting joints. (in Japanese), Mokuzai Gakkaishi (Journal of the Japan Wood Research Society), 55(3):155-162, 2009